# Modeling organic electronic materials: bridging length and time scales

Thomas F. Harrelson, Adam J. Moulé, Roland Faller

October 4, 2016

## Contents



**Abstract**

Organic electronics is a popular and rapidly growing field of research. The optical, electrical and mechanical properties of organic molecules and materials can be tailored using increasingly well controlled synthetic methods. The challenge and fascination with this field of research is derived from the fact that not only the chemical identity, but also the spatial arrangement of the molecules critically affects the performance of the material. Thus synthetic, fabrication, characterization, and computational scientists need to work closely to relate a materials performance in a device to the molecular details that cause and optimize that performance. For computational scientists in particular, the need to relate macroscopic device performance to details of molecular electronic structure brings challenges in methodology due to the need to bridge many orders of time and length scales. This article provides a survey of computational methods applied to multiple–length and time scale problems in organic electronic materials. Here we seek to highlight a few particular approaches that expand the simulation toolbox.

# 1 Introduction

Organic molecules have been recognized for their potential to harvest and emit light for device applications for decades [Morel *et al.*(1978)Morel, Ghosh, Feng, Stogryn, Purwin, Shaw, and Fishn Gleria and Memming(1976), Dyakonov and Frankevich(1998)]. Since these humble beginnings, organic light emitting diodes have become commercially available for lighting

and are widely used for display applications [Sasabe and Kido(2011), Kalyani and Dhoble(2012)]; organic photovoltaics (OPV) have achieved over 10% power efficiency [Zhang *et al.*(2016)Zhang, Ye, and Liu *et al.*(2014)Liu, Zhao, Li, Mu, Ma, Hu, Jiang, Lin, Ade, and Yan] and both small molecule and polymer semiconductors have achieved over 1 $cm^2/Vs$ mobility [Sirringhaus(2014)]. The progress represented by these astonishing technological achievements in the use of organic materials for electronic applications has come about as a result of simultaneous major advances in organic materials synthesis, capabilities in organic materials characterization, and the development of tools for organic materials modeling. This research effort is so vast that it alone could fill a library. In this review, we will highlight a subset of the research on the use of computational modeling tools used to describe the structure, dynamics, and energetics of organic electronic materials. The highlighted studies focus on modeling the semiconducting polymer poly–3–hexylthiophene (P3HT) (Figure 1a). While P3HT is not the highest performing polymer for any application, it has been more studied than any other electronic polymer and so there is a wealth of verification data to test simulated results against. Therefore, P3HT is an excellent test subject for organic electronic model development. Our goal is to examine the process of using multiple different simulation methods to simulate structure and properties. In most simulation studies, multiple modeling methods must be used in order to extract meaningful data because a single method is not able to bridge length and time scales. We will discuss limitations that can be addressed using improved modeling and verification methods. This should justify the need for further research in developing modeling tools for organic electronic materials.

Organic electronic devices and materials have become an increasingly important research and commercial area with a predicted market value of ∼$70 billion by 2026 [Das and Harrop(2015) Great Britain. Department for Business and Skills(2009), on Best Practice in National Innovation Pro Organic components are particularly valuable because molecular design allows an almost infinite variety of structures and functions to be synthesized [Cheng *et al.*(2009)Cheng, Yang, and Hsu]. Ideally, it would be possible to conduct modeling experiments to design organic molecules for electronic applications and to characterize the function of the structures using computers. However this task is currently impossible because organic electronic molecules could be crystalline or amorphous with molecular weight between $16 - 10^8$ g/mol. They could be liquids, liquid solutions, network solids, gels, or insoluble materials that are evaporated into place. They could be pure hydrocarbons, organo–metallics, metal organic frameworks, organic/inorganic nano–hybrids, biological solids, pure carbon solids and a variety of other forms. In other words, the variety of forms of organic molecules that must be described using simulations is vast. In addition, length scales from $10^{-11}$ – $10^0$ m need to be considered to cover all relevant questions from atomic arrangement to fully fabricated devices. Also time scales from $10^{-15} - 10^9$ s must be considered to cover from exciton formation to the lifetime of an organic light emitting diode (OLED) or PV device. Here we consider the subset of modeling techniques that describes structure over length scales from 0.1 – 1000 nm and dynamics over time scales from fs – $\mu$s.

One of the most important advantages of organic electronic materials is that they can be deposited from solution, which potentially makes coating over large areas very inexpensive [Krebs(2009), Krebs *et al.*(2010)Krebs, Nielsen, Fyenbo, Wadstrom, and Pedersen, Li *et al.*(2014)L Arias *et al.*(2010)Arias, MacKenzie, McCulloch, Rivnay, and Salleo]. The drawback of solution deposition is that the organic species must self–assemble into the desired molecular configuration [Moulé and Meerholz(2009), Peet *et al.*(2009)Peet, Heeger, and Bazan]. It is difficult to simulate self–assembly processes because these processes often involve

phase changes, reactions, complex interactions with the solvent and changing concentrations and temperature changes. For organic field effect transistor (OFET) materials the desired self–assembly is large molecular crystals with few defects and a particular molecular orientation [Schweicher *et al.*(2015)Schweicher, Lemaur, Niebel, Ruzie, Diao, Goto, Lee, Kim, Arlin For organic light emitting diode (OLED) materials, typically amorphous materials are desired to prevent exciton quenching. Also mixtures with low volume percentages of well spaced emitters are often desired [Sasabe and Kido(2011)]. For solution processed OPV active layers, a mixture of donor and acceptor materials is preferred [Yu *et al.*(1995)Yu, Gao, Hummelen Halls *et al.*(1995)Halls, Walsh, Greenham, Marseglia, Friend, Moratti, and Holmes]. These materials should phase separate on a length scale that maximizes exciton separation at donor acceptor interfaces while at the same time providing charge transport for holes through the donor material to the anode and for electrons through the acceptor material to the cathode [Blom *et al.*(2007)Blom, Mihailetchi, Koster, and Markov, Brabec *et al.*(2011)Brabec, Heeney, McCulloch, and Nelson].

The discovery of state–of–the–art materials used for electronic devices is achieved through combined synthesis, characterization, and simulation techniques. This is necessary to understand the morphology of the donor–acceptor mixture because we need information over different length scales, time scales, and with different contrast. For a simulation scientist, validation of a molecular model using experimental data is often the most difficult challenge because the real sample is almost always more disordered, larger, and less well defined than the simulation sample. It is often impossible to make "apples–to–apples" comparisons. Realistic models that match sample conditions can however be used to make predictions for new physics. The social challenge is develop close working relationships between simulation and characterization scientists that enable development of new modeling tools and validation using appropriate samples and methods. Here is a brief list of references for characterization techniques for organic electronic materials. Neutron scattering methods measure the structure and dynamics of hydrogen atoms in organic electronics through coherent scattering (small angle neutron scattering) and/or energy loss measurement (inelastic neutron scattering) [Pynn(2009)]. Electron microscopy and tomography create 2D and 3D images of OPV device layers with nanometer resolution [Yang *et al.*(2005)Yang, Loos, Veenstra, Verhees, Wienk, Kroon, Michels, and Janssen, Roehling *et al.*(2013)Roehling, Batenburg, Swain, Moulé, and Arslan]. Similar to neutron methods, electromagnetic radiation techniques study both the structure and dynamics of non–hydrogen atoms in organic electronics, as the atomic electromagnetic cross–section increases with atomic number. X–ray techniques such as grazing incidence wide angle scattering (GIWAXS) and small angle scattering (GISAXS) are the most useful tools to determine the spacing of molecules in ordered domains and the spacing of domains of separated materials, respectively [Salleo *et al.*(2010)Salleo, Kline, DeLongchamp, and Chabinyc]. UV/Vis spectroscopy provides information for the accessible excited electronic states of organic electronics. Infrared and Raman spectroscopy give vibrational dynamic information about the material, but selection rules prevent observation of all vibrational modes [Zahn *et al.*(2007)Zahn, Gavrila, and Salvan]. Electron spin resonance (ESR) and nuclear magnetic resonance (NMR) spectroscopies provide detailed information about the local magnetic environment of electrons and nuclei, which are used to determine molecular structure and the relaxation rates of dynamic molecular motion [Hansen *et al.*(2016)Hansen, Graf, and S Detailed reviews of characterization techniques used for OPV device and materials characterization are listed here [Chen *et al.*(2012)Chen, Nikiforov, and Darling, Huang *et al.*(2014)Huang, Kra DeLongchamp *et al.*(2012)DeLongchamp, Kline, and Herzing, Rivnay *et al.*(2012)Rivnay, Mannsfeld, M

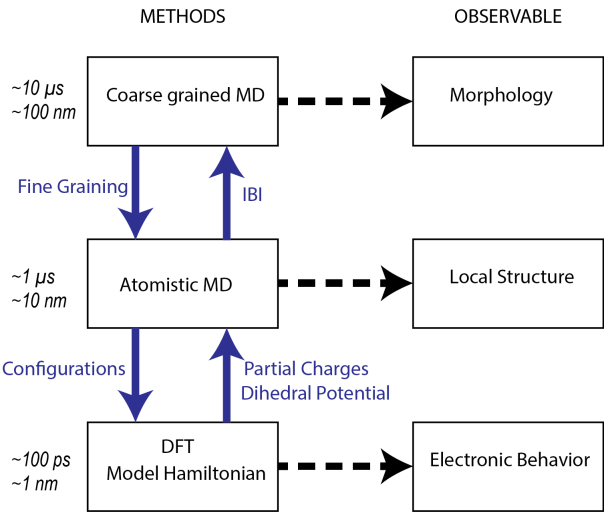


Figure 1: Flow chart that shows connection between different length/time scale simulations (left column) and the type of information gained (right column).

The experimental techniques provide a patchwork understanding of the molecular system. Simulation methods are needed to stitch together the experimental information in a consistent way, while simultaneously producing a molecular picture of the system. As with experimental characterization techniques, there are a number of modeling tools for different length and time scales [Praprotnik *et al.*(2008)Praprotnik, Delle Site, and Kremer]. In general, molecular models can be broken into three categories. First there are electronic or quantum mechanical models that explicitly treat the electron position or density separately from the nuclear position. Second there are molecular dynamics or classical models that calculate the position and forces on atoms or groups of atoms using classical force fields. Third there are continuum models that do not explicitly account for atoms, but rather keep track of densities (mass, charge etc.) and/or change in densities within a volume as a function of time. At all length scales, the methods can be used to determine a static structure or an explicit time dependence can be added to determine how a change in conditions (temperature, pressure, electric field etc) affects the molecular/electronic structure.

Modeling of organic electronic materials almost always requires the use of more than one length scale because electronic materials properties depend sensitively on the atomic/molecular structure over length scales that are not accessible using electronic simulations. Alternatively, to determine structure using classical methods, electronic simulations are needed to determine the partial charge distribution. Figure 1 shows a work flow chart that shows the interplay of different molecular simulation methods for bridging length and time scales (as will be discussed in much greater detail below). Here we show how simulations at each length scale need to be validated by measurements at the appropriate length/time scale. For example, a CG model may be validated using GISAXS or electron microscopy data. However, to explain molecular details, the CG model would need to be fine grained to the atomistic MD scale and then the molecular structure should be validated using a different technique. GIWAXS or NMR could be used to show that the MD model is consistent with measured results at the atomistic scale. If the goal of the study is to determine details of the electron transport in the simulated data a second fine graining to an electronic model would be necessary to

impart moving electrons to the nuclear positions determined using MD and within the morphology developed by CG modeling. Once again, validation of the electronic model using, e.g., pulsed spectroscopy, UPS or electronic measurements would be needed to determine that the model describes a physical reality. This process of multiple modeling and validation steps is enormously time consuming and requires many different skill sets. As a result there are very few molecular electronic samples that have been thoroughly simulated using multi–scale models. We posit here that the development of improved methods to bridge modeling techniques coupled with optimized experimental validation could greatly reduce the required effort and increase the predictive power delivered by computational methods.

# 2 Electronic Methods

Electronic structure methods are invaluable to understanding the charge transport in organic semiconductors (OSCs). The electronic structure in OSCs is locally dependent on the molecular structure and globally dependent on the electronic state distribution caused by local variations in molecular structure. Evaluating the electronic structure of a molecular system is extremely computationally demanding, meaning that only small systems (usually limited to 100s of atoms) can be treated. The electronic structure for the limit volume can only be determined for one particular conformer at one time. For highly crystalline materials, a small set of atoms is usually sufficient to characterize a material in silico using electronic structure methods and the assumption that the structure has no variations over a large sample volume is a good one [Feng *et al.*(2013)Feng, Wang, Zheng, Zhang, Fan, Liu, Amoureux, and Deng, Usta *et al.*(2011)Ust This is called the infinite crystal approximation. Most high–performing OSCs are locally disordered [Venkateshvaran *et al.*(2014)Venkateshvaran, Nikolka, Sadhanala, Lemaur, Zelazny, Kepa, H where the disorder introduces a large variety of molecular conformers that cannot be simulated using symmetric boundary conditions. Thus the length scale or number of conformers is much larger than can be feasibly simulated. Electronic structure methods are still useful because they provide molecular scale electronic information to parameterize larger models. When materials are disordered, these simulations fail to account for the structural heterogeneity found in most samples such that a sufficient number of possible conformers need to be calculated. Thus a clever choice of sample configurations is needed to extract meaningful electronic simulation results.

Electronic structure methods can be grouped into two main categories: ab initio and semi–empirical methods. Ab initio methods do not require external parameters other than atomic positions to complete the calculation, whereas semi–empirical methods have fitting parameters. Within these two categories, we focus on density functional theory (DFT) and tight–binding Hamiltonian methods.

## 2.1 Density Functional Theory

Density functional theory presents a computationally efficient way to approximately solve the many–body Schrödinger equation, actually the Kohn–Sham equation. The efficiency of DFT comes from the collapse of a high–dimensional many body problem (positions of every electrons represented as variable) into a simpler problem of a self–consistent electron density equation. The set of self–consistent equations solved in DFT are below (Equations 1 - 3). Equation 1 is an effective single body equation for a single

orbital, $\phi_i$, which is formed by an effective single body potential ($V_s$) containing all the repulsive forces from the other charges. Equation 2 defines the electron density, $n$, as the sum of the individual orbital densities. The effective single body potential, $V_s$, contains contributions from three terms: the external potential ($V$), the electron–electron repulsion, and the exchange–correlation potential ($V_{XC}$). $V_{XC}$ has no classical meaning, and is a consequence of mapping a quantum mechanical many–body problem onto an effective single body system. The exchange–correlation potential is the functional derivative of the exchange–correlation (XC) functional with respect to electron density, which means the functional is invariant to changes in the system configuration. Thus, in order to solve the equations for DFT for any system, we must specify the form of the exchange–correlation functional. Finding the exact form of the exchange–correlation functional would be solving the full many body problem, but several approximate functionals exist, which provide many flavors of DFT that are optimized for different problems [Becke(1993), Yanai *et al.*(2004)Yanai, Tew, and Handy, Paier *et al.*(2005)Paier, Hirschl, Marsman, and Kresse].

$$\left[\frac{-\hbar^2}{2m}\nabla^2 + V_s(\vec{r})\right]\phi_i(\vec{r}) = \epsilon_i\phi_i(\vec{r}) \quad (1)$$

$$n(\vec{r}) = \sum_i^N |\phi_i(\vec{r})|^2 \quad (2)$$

$$V_s(\vec{r}) = V(\vec{r}) + \int \frac{e^2 n(\vec{r'})}{\left|\vec{r} - \vec{r'}\right|} d\vec{r'} + V_{XC}(\vec{r}) \quad (3)$$

The information contained in the electronic structure provides insight into the structure (and in the case of time dependent DFT or Car–Parinello MD) dynamics of the nuclei. The Hellman–Feynman theorem provides a connection between the inter–atomic forces and DFT equations allowing the computation of equilibrium positions or nuclear dynamics using time–dependent simulations. Combining the computation of inter–atomic forces and a optimization scheme such as steepest descent, produces an optimized geometry in a local energetic minimum. Geometry optimizations have been applied to OSCs to find static equilibrium states of organic electronic oligomers and/or dopants [Zhu *et al.*(2011)Zhu, Kim, Yi, and Brédas]. If coupled with a molecular dynamics scheme, DFT can reasonably accurately simulate the dynamics of molecules, including non–equilibrium geometries [Goldman *et al.*(2009)Goldman, Reed, Kuo, Fried, Mundy, and Curioni]. However, the computational expense required for computing inter–atomic forces using DFT limits the ability of these schemes to properly sample phase space in all but the simplest systems.

Technically the calculations need a basis to the vector space of orbitals (or electron density distributions). The simulation can be tailored to specific molecular systems through the choice of an appropriate basis set. Gaussian basis sets are used to describe molecule(s) in the gas phase. If the dielectric of the background is adjusted, the conditions mimic an implicit solvent, which extends the use of Gaussian basis sets to the liquid phase. Deficiencies of this approach include the absence of neighbor interactions, and the computational expense of DFT limits polymer simulations to oligomers (as one can feasibly simulate 100s of atoms). Plane wave basis sets are used to model extended crystalline solids due to the periodicity of the basis functions [Feng *et al.*(2013)Feng, Wang, Zheng, Zhang, Fan, Liu, Amoureux, and Deng,

Usta *et al.*(2011)Usta, Facchetti, and Marks], but again computational cost limits the unit cell size. However, neighbor interactions are included and infinitely long crystalline polymers can be simulated. However, disordered systems remain difficult to model due to the inability to include multiple conformers within one unit cell and the small size of the unit cell mandates an artificial symmetry.

Rigorous experimental validation of DFT methods is crucial due to the number of assumptions. Common experiments used to validate electronic simulations include ultraviolet photoelectron spectroscopy (UPS) [Braun *et al.*(2009)Braun, Salaneck, and Fahlman, Ludwigs(2014)], ultraviolet–visible spectroscopy (UV–vis) [Vanlaeke *et al.*(2006)Vanlaeke, Swinnen, Ha Winokur *et al.*(1989)Winokur, Spiegel, Kim, Hotta, and Heeger, Tapping *et al.*(2015)Tapping, Clafton and infrared spectroscopy (IR) [Winokur *et al.*(1989)Winokur, Spiegel, Kim, Hotta, and Heeger, Yin *et al.*(2016)Yin, Wang, Fazzi, Shen, and Soci, Yuan *et al.*()Yuan, Zhang, Sun, Hu, Zhang, and Du Each experiment validates a different observable of the DFT calculation. UPS provides the energy levels of the valence electrons in the ground state, which can be accurately calculated using DFT. UV–vis measures the energy differences between excited electronic states and the ground state. This is difficult to reproduce with DFT; it is difficult to assign meaning to excited orbitals in DFT, as the theorems of DFT hold for the ground state only [Eschrig(2003)]. IR spectroscopy measures symmetry allowed molecular vibrations, which can be accurately simulated by finding the eigenvalues of the a matrix of interatomic force constants [Yin *et al.*(2016)Yin, Wang, Fazzi, Shen, and Soci, Yuan *et al.*()Yuan, Zhang, Sun, Hu, Zhang, and Duan].

In all cases, the ease of validation is determined by the complexity of the material. Heterogeneous materials, such as semicrystalline P3HT, have intermixed crystalline and amorphous domains. Crystalline domains simulated using DFT must be perfectly periodic, meaning that only single crystal systems are well suited for DFT simulations. If the system is composed of randomly ordered crystallites, plane wave DFT will over–estimate alignment of dipoles, quadrupoles, etc. This is problematic because most OSCs have a significant quadrupolar moment [Poelking *et al.*(2015)Poelking, Tietze, Elschner, Olthof, Hertel, Baumeie Thus, theorists are presented with the options of underestimating (Gaussian DFT) or overestimating (PW–DFT) environmental electrostatic effects. Reducing the effect of these assumptions in crystalline domain OSC simulations represents an ongoing challenge for DFT method development[Poelking *et al.*(2014)Poelking, Daoulas, Troisi, and Andrienko]. As discussed above, to simulate amorphous domains a huge number of different molecular configurations would need to be addressed. Instead particular configurations are simulated and assumed to provide meaning to the sample in general. Only a wise choice of characteristic simulations makes the simulation meaningful for the sample.

DFT with Gaussian basis sets has been used to study charge–transfer states between dopants and OSCs providing a link between polymer length and the amount of charge transferred from the OSC molecule to the dopant [Zhu *et al.*(2011)Zhu, Kim, Yi, and Brédas, Di Nuzzo *et al.*(2015)Di Nuzzo, Fontanesi, Jones, Allard, Dumsch, Scherf, Von Hauff, Schumacher, an Figure 2.1 demonstrates the effect of molecular geometry on charge transfer between quatro–thiophene and the dopant F4TCNQ. Different charge–transfer configurations display changes in amount of fractional charge transfer. At experimental temperatures, we expect multiple instances of each configuration present in Figure 2.1, which demonstrates the importance of sampling multiple configurations when relating DFT simulation results to OSC properties. In addition to charge–transfer properties, Gaussian based DFT can be used to parameterize classical molecular dynamics models [Do *et al.*(2010)Do, Huang, Faller, and Moulé and model Hamiltonian based schemes [Lee *et al.*(2015)Lee, Aragó, and Troisi]. Molecu-

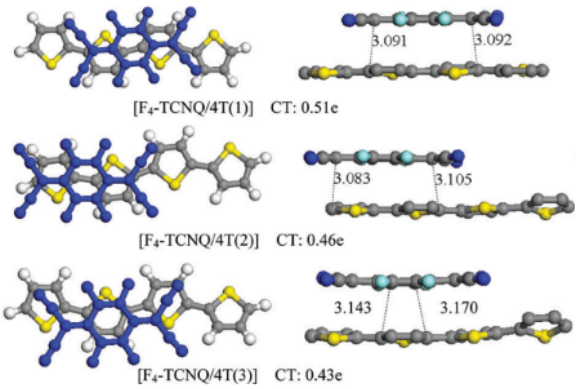


Figure 2: B3LYP-D/6-31+G(d)-optimized geometries of the F4TCNQ/4T complex at three energy minima (top view, left; side view, right). Interatomic distances between two molecules (in Å) and the amount of charge transfer, CT, are shown. For clarity, hydrogen atoms are not shown in the side views.

lar dynamics simulations require an estimation of partial atomic charges, and the potential arising from the nuclei and the electron density (determined from DFT simulations of a particular conformer) is fit to an effective electrostatic potential originating from non–integer charges centered at the nuclear positions [Breneman and Wiberg(1990)]. Since the electron density is unique to the nuclear positions, the effective partial charges may change upon nuclear rearrangement, which is problematic for molecular dynamics as the partial charges are fixed for all configurations. This means that the choice of molecular conformer used for the DFT simulation can have a large effect on the partial charges and accuracy of the molecular dynamics model.

## 2.2 Model Hamiltonian Methods

DFT based methods are cumbersome when studying the electron dynamics of complex molecular systems. Poor computational scaling of DFT severely limits system size, which means electron dynamics can only be studied on the length scale of nanometers.

To reduce the computational expense, many groups turn to model tight–binding Hamiltonians to simulate the quantum dynamics of electrons without explicitly accounting for the positions of the nuclei. A tight–binding Hamiltonian is a matrix of interactions between neighboring states (commonly referred to as coupling between states). An example of a model Hamiltonian is provided in equations 4–7 [Lee *et al.*(2015)Lee, Aragó, and Troisi]. This set of equations modifies the typical tight–binding Hamiltonian (equation 5) to include coupling to a bath of phonons. In this example, $\epsilon$ is the on–site energy of the electron, $\tau$ allows hopping between adjacent sites, and $\lambda/\alpha$ allow local/nonlocal transfer of electron energy to vibrational modes. $|i\rangle$ represents an electronic state, whose form is not clearly defined, but it can be assumed that the set of all states are orthonormal. Equation 7 represents the energy from classical harmonic oscillators represented in the phonon modes of the system. The expansion of a complex Hamiltonian into a series of interaction potentials/energies allows one to identify parameters responsible for changes in electron dynamics. These parameters can be attributed to the chemical structure of the underlying molecules in the material, which provides insight into potential molecular design rules.

$$\hat{H}_{total} = \hat{H}_{el} + \hat{H}_{el-ph} + \hat{H}_{ph} \tag{4}$$

$$\hat{H}_{el} = \sum_{i}^{N} \left[ \epsilon \left| i \right\rangle \left\langle i \right| + \sum_{j=i\pm1} \tau \left| i \right\rangle \left\langle j \right| \right] \tag{5}$$

$$\hat{H}_{el-ph} = \sum_{k} \sum_{i}^{N} \left[ \lambda^{(k)} u_i^{(k)} \left| i \right\rangle \left\langle i \right| + \sum_{j=i\pm1} \alpha^{(k)} \left( u_i^{(k)} - u_j^{(k)} \right) \left| i \right\rangle \left\langle j \right| \right] \tag{6}$$

$$\hat{H}_{ph} = \sum_{k} \sum_{i}^{N} \left[ \frac{1}{2} m^{(k)} \left( \dot{u}_i^{(k)} \right)^2 + \frac{1}{2} m^{(k)} \left( \omega^{(k)} u_i^{(k)} \right)^2 \right] \tag{7}$$

In the context of OSCs, an electronic state (a single wave–function) rests on a molecular "site", but the actual wave–function is never computed. Coarse graining a set of nuclear positions to represent an electronic site limits the specificity of the model for a particular sample. When applied to OSCs, model Hamiltonians typically set the on–site energies ($\epsilon$) and various coupling energies ($\tau$) between electronic sites to be constant, which may be parameterized using DFT. The coupling constants allow the electrons to hop from one site to another, and are given by the overlap of the wave–functions between sites. However, the static and dynamic disorder of OSCs requires the on–site energies and coupling constants to vary to account for energetic variation between sites due to different molecular environments and/or molecular vibrational motion (phonons). To approximate disorder, the on–site energies and coupling constants have been randomized around a mean value [Noriega *et al.*(2013)Noriega, Rivnay, Vandewal, Koch, Stingelin, Smith, Toney, and Salleo, Fornari and Troisi(2014), Spano(2005), Tapping *et al.*(2015)Tapping, Clafton, Schwarz, Kee, and Huan Recently, coupling to vibrational modes and a thermal bath have been added to model Hamiltonian approaches to test the effects of dynamic and static disorder on electronic dynamics [Lee *et al.*(2015)Lee, Aragó, and Troisi].

Lee et. al. provide an example of a model Hamiltonian approach applied to OSCs to explain the charge separation through quantum diffusion [Lee *et al.*(2015)Lee, Aragó, and Troisi]. Figure 3 shows a schematic of what the model Hamiltonian represents, which is accompanied by some relevant results. Initially an electron is placed at position 2, which is separated from the positive charge by 26 Å. At short times ($\sim$ 100 fs), the electron quickly separates from the charge before settling into the lowest energy state at longer times ($\sim$ 10 ps). The important result is that a portion of the electron density separates quickly from the positive charge, while the remainder of the density moves toward the positive interface. This charge density bifurcation can be explained by conservation of average energy within the electronic Hamiltonian; the system lowers its energy by moving the electron density closer to the positive interface, but this must be balanced by a portion of density moving away from the interface to conserve energy. Without electron–phonon coupling, this bifurcation is effectively coherent in opposite directions. Inclusion of electron–phonon coupling and vibrational energy into the Hamiltonian reduces this outward motion, as the inclusion of other energy types destroys the conservation of electronic energy. High energy electronic eigenstates couple to low energy states through phonons, allowing electronic relaxation, which decohere the electronic density over time. The strength of the electron–phonon coupling governs this decoherence, and reduces the charge separation efficiency. The authors assume only one high and one low energy mode, and electron–phonon coupling only exists between the high energy mode, which prevents quantitative conclusions. In all cases, the authors were able to show fast charge separa-

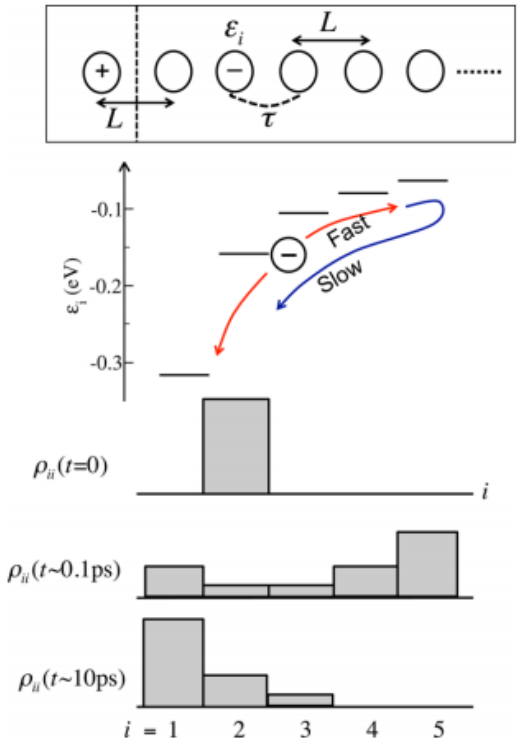


Figure 3: *Top panel:* Schematic of a one–dimensional acceptor lattice model. *Central panel:* corresponding on-site energy $\epsilon_i$ (L = 13 Å and $\epsilon/\epsilon_0 = 3.5$). The arrows indicate short time quantum diffusion and long time relaxation toward the lowest energy site. *Bottom panel:* Schematics of time evolution of charge density along acceptor sites. Used with permission from [Lee *et al.*(2015)Lee, Aragó, and Troisi].

tion, and slow relaxation to thermal equilibrium, leading them to conclude that the yield of free charges is governed by the interplay of those two competing processes.

The accuracy of model Hamiltonian approaches critically depend on the accurate parametrization of the energies and coupling constants. This parametrization is non–trivial with the inclusion of vibrational coupling, which, in principle, introduces $\sim 3N$ parameters for each type of vibrational coupling considered, where $N$ is the number of atoms in the solid. The parametrization can be simplified as many vibrational modes are roughly equivalent. However, the smallest possible unit cell of crystalline P3HT contains 100 atoms (294 vibrational modes), which makes parametrization difficult and time consuming. Additionally, the lack of information on atomic positions precludes the sampling of different disordered configurations typically seen in polymeric OSCs. To properly understand disordered configurations present in most OSCs, a method accounting for atomic degrees of freedom is required. To mitigate the computational scaling limitations of electronic modeling, one must use molecular dynamics methods.

# 3 Classical Simulation Methods

## 3.1 Molecular Dynamics

Molecular dynamics is a method that tracks the classical motion of a particle based system following Hamilton's equations according to a (semi–)empirical force field. The position of every interaction site (in the case of an atomistically detailed model an atom) at every time step is known, providing complete information about the system. The use of a semi–empirical force field in a classical scheme improves computational performance due to the elimination of electronic degrees of freedom, allowing the simulation of $10^5$ atoms or more for up to microseconds. The massive amount of information is used to generate statistical mechanical ensembles and from there the macroscopic properties of the system, which provide a clear path to compare simulation to experimental results. In the context of OSCs, electrical properties are of primary interest, which are not directly available from MD simulations because electron dynamics is not included in the simulation. Thus, MD simulation results are commonly combined with electron dynamics methods, such as semiclassical Marcus theory, to create electronic properties from the structural results of MD. In this section, we discuss the fundamentals of MD, and some relevant examples of how MD provides significant insight into the understanding of electrical properties of OSCs.

A good comparison between experiment and theory requires a well parameterized force field. The force field typically contains the partial charges, dispersion force parameters, and bond constants for stretching, angle bending, and dihedral motion. The partial charges and some bonded parameters are often parameterized from DFT methods, whereas the dispersion parameters are optimized from empirical data although DFT can also been used [Sha and Faller(2016)]. Care must be taken when parameterizing partial charges from DFT, as long range electrostatic effects (not accounted for in DFT) have a strong effect on the electronic structure in highly ordered organic electronics [Poelking *et al.*(2015)Poelking, Tietze, Elschner, Olthof, Hertel, Baumeier, Wuerthner, Meerholz, L
Also, the partial charge distribution can be skewed by choosing a single molecular conformer in DFT that does not represent all of the possible conformers in a sample. For example, a fully planar conjugated chain may be used to determine the partial charge distribution, but only a fraction of the chains in the sample may have this fully pla-

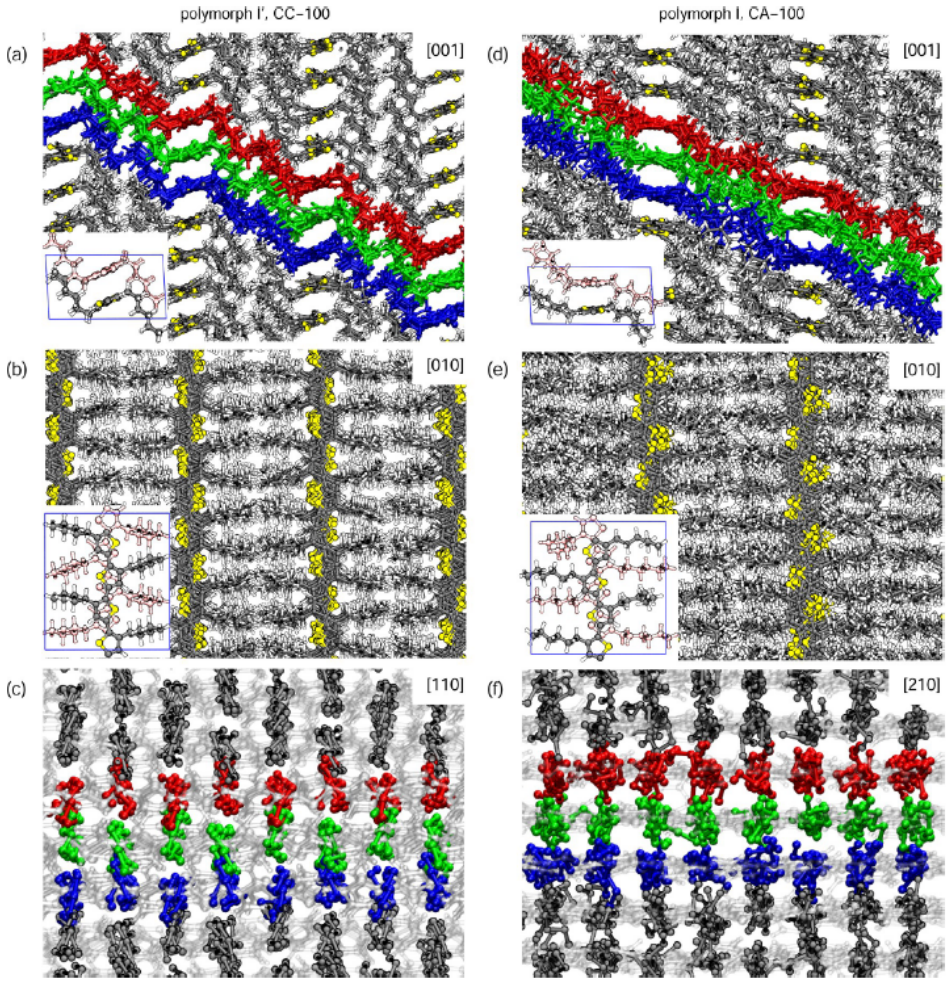


Figure 4: Regioregular poly(3-hexylthiophene) lamellar crystals of polymorphs I′ (a-c) and I (d-f) as obtained from molecular dynamics simulations. Projections are constructed along the (a, d) [001], (b, e) [010], (c) [110], and (f) [210] crystal direction. Note the degree of interlamellar correlation mediated by the hexyl side chains even in their disordered phase. Reprinted from [Poelking *et al.*(2015)Poelking, Tietze, Elschner, Olthof, Hertel, Baumeier, Wuerthner, Meerholz,

nar configuration. Also as a partial charge does not relate to a operator in quantum–mechanical sense there is ambiguity in the way to map the electron distribution onto partial charges. Since the partial charges remain fixed throughout the duration of the MD simulation, the chosen DFT configuration will affect the structures and dynamics sampled using the MD model. To complicate this issue, organic electronic molecules can become polarized or interacting donor–acceptor pairs can transfer charge at heterojunctions. These intermolecular electronic interactions dynamically change the partial charges in the system, limiting the applicability of classical MD methods. Also, in films of pure P3HT, we see differences in the UV–vis spectrum as a function of dihedral stiffness, indicating that partial charge may also be a function of the intermonomer dihedral angle [Niles *et al.*(2012)Niles, Roehling, Yamagata, Wise, Spano, Moulé, and Grey].

Poelking and Andrienko studied the stability of the crystalline phase of P3HT using MD [Poelking *et al.*(2015)Poelking, Tietze, Elschner, Olthof, Hertel, Baumeier, Wuerthner, Meerholz,

to address the solid/solid phase transition from the metastable I′ polymorph to the more thermodynamically stable form I of P3HT [Yuan *et al.*()Yuan, Zhang, Sun, Hu, Zhang, and Duan, Dudenko *et al.*(2012)Dudenko, Kiersnowski, Shu, Pisula, Sebastiani, Spiess, and Hansen]. Figure 3.1 shows sample configurations for polymorph I′ (a-c) and polymorph I (d-f). The MD simulations show that increasing temperature causes an irreversible transition from polymorph I′ to I, indicating that polymorph I is thermodynamically favored and should be present in P3HT films at relevant temperatures. Experimentally, it is difficult to distinguish between the two structures [Prosa *et al.*(1992)Prosa, Winokur, Moulton, Smith, and Heeger, Kayunkid *et al.*(2010)Kayunkid, Uttiya, and Brinkmann, Brinkmann and Rannou(2009)], due to the significant structural disorder at the atomic scale and similar spacing between parallel polymer backbones. In this example, MD is used to provide structural and thermodynamic information that is unobtainable from experiments. The downside is that the results are only as reliable as the assumptions made in the MD model.

After finding the molecular trajectories with MD, Poelking and Andrienko fed the simulated morphologies into a semiclassical Marcus hopping scheme allowing the estimation of electronic transport behavior. The electronic transport behavior provided estimates for charge mobilities that showed excellent agreement with experiments in P3HT nanofibers. Specifically, they show how a few defects in side–chain attachment (90% regioregular P3HT) lead to an order of magnitude drop in charge–carrier mobility [Poelking and Andrienko(2013)]. This study shows how classical molecular dynamics can be coupled with an electronic dynamics scheme (semiclassical Marcus theory) to provide electron dynamics at longer length scales than is possible using DFT alone. This approach is limited by the assumptions made to simulate electron dynamics at this length scale; the system is effectively an infinitely large crystal with chain ends occurring every 20 monomers. Films of P3HT have randomly oriented crystallites embedded within amorphous domains. The long chains can wrap into several crystalline domains or the same domain several times, meaning that a single chain has both amorphous and crystalline components. This structural heterogeneity was not considered in this study due to the increased computational expense that simulation of the more disordered system would entail.

In a similar study, Alexiadis et al used atomistic MD to study self–organization and structure in (semi)crystalline rr–P3HT by addressing the amorphous and crystalline parts separately. Within the crystalline region, a unit cell that looks similar to polymorph I′ is the dominant structural moiety at room temperature [Alexiadis and Mavrantzas(2013)]. The reason for the differences in reported structure from Poelking et al is the different force field, which highlights the importance in carefully choosing/parameterizing the force field from DFT and validating with measured data.

Atomistic molecular dynamics of P3HT and PBTTT–C12 were compared by our group to clarify why nanoscale structural properties lead to higher measured hole mobility in PBTTT versus P3HT [Do *et al.*(2010)Do, Huang, Faller, and Moulé]. We found that the dihedral angle between the two thiophenes in PBTTT is more planar than that in P3HT, while the thienothiophene dihedral in PBTTT displayed similar variation to P3HT. The bulkier side chain in PBTTT increases antiparallel order between intra–chain monomers relative to P3HT, which produces a structure with fewer defects. In this case we did not directly calculate how the dihedral angles of the polymer backbone effect the charge mobility but rather inferred this data from the structure. The increased order and the net increase in backbone planarity are the likely causes for higher electrical mobilities in PBTTT. Our simulation also allowed us to predict that the variation in the

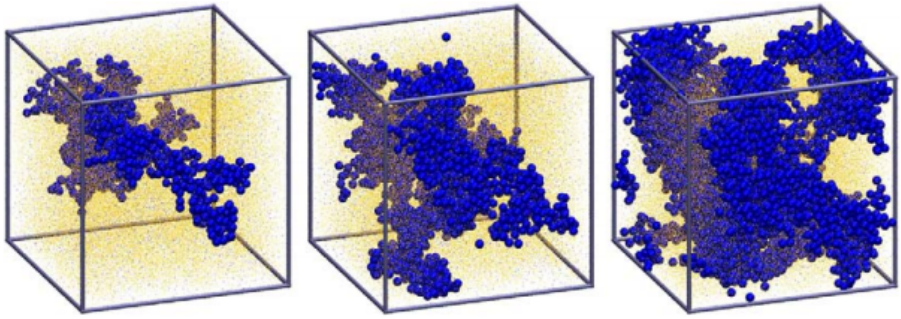

Figure 5: Snapshots of the simulation configuration of the system with P3HT:$C_{60}$ = 1.27 : 1 (w/w) with $N_{mono} = 48$ at $t = 0$ ns (left), $t = 30$ ns (center), and $t = 135$ ns (right). The $C_{60}$ molecules in the largest cluster are highlighted in blue and all other particles in the system are shown as dots. The length of each side of the simulation box is roughly 25 nm. (For interpretation of the references to color in this figure legend, the reader is referred to the web version of this article.) From [Huang *et al.*(2011)Huang, Moulé, and Faller]

thienothiophene–thiophene dihedral angle can be reduced with attachment of a small side chain to increase rotational inertia making deformation less likely. The advantage to this approach is reduced computational expense because we did not need to calculate transfer integrals. The disadvantage is lack of quantitative data and an inability to validate to electronic data.

As mentioned above, classical MD does not allow dynamic change of partial charges which means that the charge cannot react to its local environment or other charges. As a result it is not possible to simulate fully the dynamic processes for charged sites, like the diffusion of a dopant molecule or reaction dynamics like formation of a cross linked bond. Future MD will need to include polarizable or even reactive modeling to expand the modeling tool kit. A second challenge is to model structure formation which is currently limited for classical MD in condensed matter due to both lack of structure sensitive force fields or access to long time and length scales. MD is limited to at best microseconds, which is not long enough to observe structure formation, particularly in polymers. To sample longer times, we must reduce degrees of freedom, which requires coarse–grained methods.

## 3.2 Coarse Grained Modeling

As described above, MD modeling allows simulation of molecular structure over longer length and time scales larger than electronic models make possible, but at the cost of force fields that are not sensitive to molecular conformation. Box sizes with tens of nm can be simulated for up to microseconds using MD. However many processes occur over longer length scales and take much longer. One example is the formation of a crystalline domain from a polymer melt. In order to describe and model these slow processes, it is necessary to perform molecular dynamics on groups of atoms that are connected and have similar function. For example, a benzene ring can be modeled as a single coarse grained (CG) "superatom". Thus a CG–MD model has fewer particles with less chemical specificity, but can be used to model larger volumes for longer time periods.

A few years ago our group developed a model for P3HT and P3HT/$C_{60}$ mixtures based

on systematic coarse–graining using the Iterative Boltzmann Inversion (IBI) Method where a few heavy atoms — typically 4–6 — together with their hydrogens are subsumed into a "superatom" [Huang *et al.*(2010)Huang, Faller, Do, and Moulé]. The interactions between these superatoms are optimized that local structure (as defined by pair correlation functions, superbond distances etc.) is correctly represented and at the same time simulations are several orders of magnitude faster to allow the study of morphology of polymer/fullerene bulk heterojunctions at length and time scales relevant to organic photovoltaic devices. These models although optimized at only one state–point each correctly represent the structure of the systems in a sizable range of state space although that is not guaranteed a priori [Sun *et al.*(2008)Sun, Ghosh, and Faller].

A variation of the model using the same IBI methodology was used by the Huang group to study the aggregation of P3HT into high–aspect–ratio nanofibers, nanowires, or nanoribbons in implicit weak solvents such as anisole. The CG model was adapted to the local structure and dynamics of an atomistic model with explicit solvent. The simulations match the experimental phase behavior of P3HT in anisole as they yield aggregation below ≈320 K but not above. At room temperature hairpins and helices of single chains are predicted. These single chain conformations are the building blocks for the larger scale structures. These simulations are particularly interesting because they, for the first time, used polymers with molecular weight similar to experiment and also showed hairpin folding on the same length scale as seen in experiment. Further the helix structure has not been experimentally detected, as so is a theory driven prediction. In addition to providing insight into this mechanisms of fiber formation, the simulations can also resolve details of the molecular–level organization in the fibers [Schwarz *et al.*(2013)Schwarz, Kee, and Huang]. So this approach shows several advantages in moving to longer length and time scales, allowing formation of realistic molecular structures that are found in P3HT anisole and toluene solutions[Niles *et al.*(2012)Niles, Roehling, Y
But these CG models are devoid of fine structure or electronic information. Similar to polystyrene [Bayramoglu and Faller()] CG models of P3HT validated in either in dilute solution or polymer melts can be used to show structure formation with a high degree of accuracy. This observation shows that CG models can be used outside of the original state-point. In this case the P3HT was coarse grained from a melt but folded to make a crystalline solid in a dilute solution.

In further work the Huang group used the dihedral angle distribution in the CG P3HT clusters to predict exciton hopping under the assumption that the longest straight segments would represent the lowest energy configuration [Tapping *et al.*(2015)Tapping, Clafton, Schwarz,
Although the atomistic details were missing in the CG model, the modeled exciton hopping kinetics were similar to data acquired using ultra-fast laser techniques in clusters of P3HT in solution, validating the use of a CG model to extract electronic information. In a second extension of the CG model, the Huang and Groves developed mixtures of P3HT at different MW averages and distributions [Jones *et al.*(2016)Jones, Huang, Chakrabarti, and Groves]. In this study, nanocrystal formation in a melt was predicted from different MW distributions. The CG morphology was fine grained to the atomistic scale and then the atomistic geometries were used with a kinetic Monte Carlo method to determine charge transport characteristics of the semicrystalline P3HT morphologies. The crystalline structure was used to validate the simulation at the atomistic scale. This study completed the entire work flow diagram shown in Figure 1. The P3HT was modeled from DFT, the partial charges were used in atomistic MD, the atomistic MD was then coarse grained and high MW morphologies were obtained over long length and time scales. The morphology was

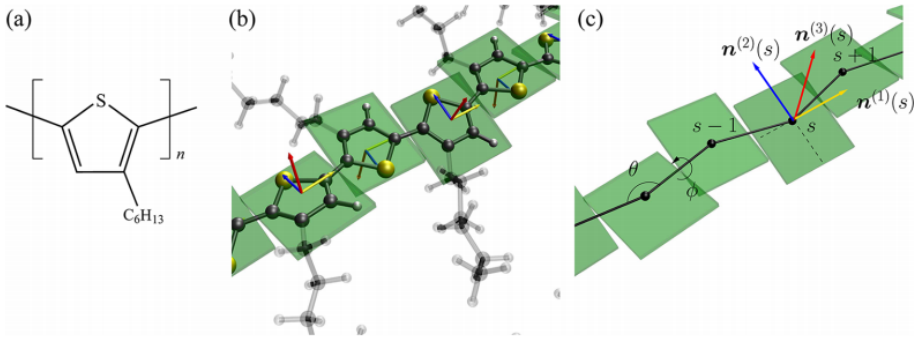


Figure 6: (a) Chemical structure of poly(3-hexylthiophene) (P3HT). Atomistic (b) and coarse-grained (c) representations of the P3HT chain. In the coarse-grained model each repeat unit is a single interacting site placed at the intersection of two imaginary lines placed along the bonds connecting the thiophene rings. This choice improves the transferability of the coarse-grained potential.; Reprinted from [Gemünden *et al.*(2013)Gemünden, Poelking, Kremer, Andrienko, and Daoulas]

then fine grained to the atomistic scale and finally the nuclear positions were used for charge transport calculations. At each step, over six years the models were validated.

A more generic coarse–grained model can also be developed for describing the liquid crystalline like order in P3HT on the mesoscale [Gemünden *et al.*(2013)Gemünden, Poelking, Kremer, A The bonded interactions were also here obtained by Boltzmann–inversion from the atomistic scale under $\Theta$–solvent conditions which produces the same single chain statistics like a melt. The non–bonded interactions are anisotropic and soft. They stem from a combination of $\pi - \pi$ interactions and the entropic repulsion between side chains. This model obtains uniaxial and biaxial nematic mesophases, where molecular weight effects on phase behavior are correctly represented. Conjugation defects tend to localize near chain ends [Gemünden *et al.*(2013)Gemünden, Poelking, Kremer, Andrienko, and Daoulas]. Such a model is not as chemically accurate as a systematically coarse–grained model. However, due to the generic nature such models allow to control fundamental physical or chemical properties in the model and therefore study their influence.

**Chemistry vs Morphology** Jayamaran and her group have performed a series of large scale CG simulations to study the morphology of P3HT–like systems with different chemical identity using a simplified version of our IBI derived model [Jankowski *et al.*(2013)Jankowski, Marsh, Marsh *et al.*(2014)Marsh, Jankowski, and Jayaraman]. They present a high–throughput coarse–grained simulation study that links molecular–level parameters to large scale morphological features in pure polymers and donor–acceptor blends. For the polymers they vary the arrangement of the sidegroup as they study systems with isotactic, syndiotactic and double–syndiotactic (switching sides every two groups) arrangement of side groups. This is supposed to mimic P3HT, PBTTT and PDHTB. Figure 7 shows simulated morphologies for P3HT and PDHTB along with simulated GIWAXS data and measured GIWAXS data. This is an excellent example to show how simulation data can be validated against measured data. In these examples, the backbone and side chain of the polymer phase separate more than would be expected in a measured sample. The simulated spectra are lower resolution because the volume of the simulated data is much lower than the volume of the experimentally measured sample

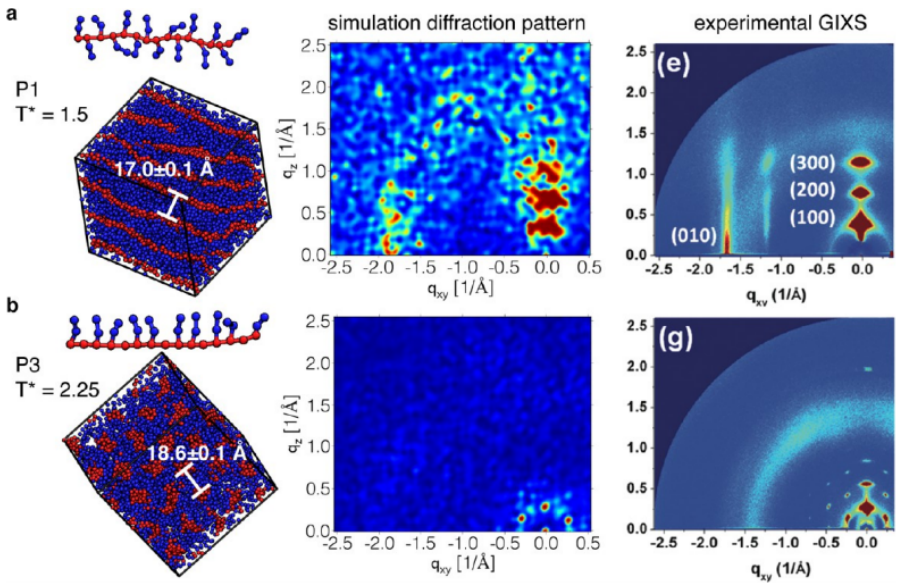


Figure 7: (a) Imperfect lamellar P1 (left), diffraction pattern calculated from simulation data (center), and GIWAXS data from annealed P3HT (right). (b) P3 in hexagonally packed cylinders at T* = 2.25 (left), diffraction pattern calculated from simulation data (center), and GIWAXS data from annealed PDHBT (right). Experimental diffraction patterns adapted with permission from ref 46.; Reprinted from [Jankowski *et al.*(2013)Jankowski, Marsh, and Jayaraman]

For the blends of the simulated polymers with fullerenes, they vary the miscibility of the acceptor by changing the non–bonded parameters of the acceptors with the donors as well as other acceptors. They are able to obtain a variety of morphologies including lamellae, hexagonally packed cylinders, and acceptor intercalation among donor side chains. There is also an order disorder transition (ODT) below which short chains self–assemble into lamellae or close packed cylinders. Based on the simulated results, design parameters can be made for how to tailor blend morphologies by changing the local chemistry. The layer spacings in their morphologies generally agree with experimental data. The average center–to–center distance in hexagonal morphology for the PDHTB variant is smaller than experimentally observed [Ko *et al.*(2012)Ko, Hoke, Pandey, Hong, Mondal, Risko, Yi, Noriega, Mc
But the model is able to explain the existence or non–existence of the cylindrical morphology for the different structures as alternating side–chain orientations inhibit cylindrical packing.

In a separate publication, they determined a phase diagram for melts of thiophene oligomers with different side chain attachments. Depending on chemistry, disordered systems, lamellae, perforated lamellae, cylinders, and ribbons could be formed. Oligomer architecture affects also the ODT because backbone beads are the species with the strongest enthalpic driving force for aggregation, and the different architectures permit different amounts of backbone bead exposure [Marsh *et al.*(2014)Marsh, Jankowski, and Jayaraman]. This clearly shows the strength of experimentally validated CG simulations as the design rules determined here can be used by polymer synthesis groups to predict the effect of chemistry on morphology formation of complex polymer systems.

Root et al. use coarse–grained molecular dynamics simulations to predict a number of

mechanical properties – tensile modulus, Poisson ratio – for P3HT and its blend with $C_{60}$. It turns out that the degree of coarse–graining has a strong effect on the predicted properties as a one to one mapping (one 3–hexylthiophene per bead) leads to inaccurate density and modulus values. A three–site model like proposed by Huang [Huang *et al.*(2010)Huang, Faller, Do, a leads to values which are in reasonable agreement with experiments. For longer chains where entanglements play a role a decrease of the entanglement density with increased blending concentration of fullerene is observed which might explain the experimental embrittlement [Root *et al.*(2016)Root, Savagatrup, Pais, Arya, and Lipomi].

Du et al use Dissipative Particle Dynamics (DPD) with a rather simple potential of the standard P3HT/PCBM system to determine the 3D morphology of BHJ solar cells [Du *et al.*(2015)Du, Ji, Xue, Hou, Tang, Lee, and Li]. Then, they estimate the performance using graph theory. They find that a volume fraction of about 40-50% PCBM is optimal and leads to a bi–continuous morphology with about 6 nm domain sizes. They also study the effect of processing conditions on the morphology where they find that 413 K is the optimal temperature and that the degree of phase separation between polymer and fullerene increases during evaporation, i.e. the solvent weakens the phase separation. In spite of these seemingly predictive results, the CG model in this study does not produce a morphology consistent with P3HT/PCBM. P3HT is a semicrystalline polymer and the crystalline domains at immiscible with PCBM while the amorphous domains mix with PCBM. So the mixed morphology is either two or three phased depending on whether there is enough PCBM to fill the amorphous P3HT volume.[Yin and Dadmun(2011), Müller *et al.*(2008)Müller, Ferenczi, Campoy-Quiles, Frost, Bradley, Smith, Stingelin-Stutzmann, and Roehling *et al.*(2013)Roehling, Batenburg, Swain, Moulé, and Arslan] The cited DPD model generates a two phase morphology at all mixing ratios and thus produces morphologies that are bi–continuous but not physically relevant to P3HT. This is an example in which a model was insufficiently validated by published data.

Clearly the extension of simulation techniques over multiple length scales leads to increased prediction power. However the cost in scientific and computational time is large. For a CG simulation, first an electronic model of the polymer must be developed and validated. Then the partial charges are used to create a molecular scale MD model, which must also be validated by experiment. Then IBI (or another technique like force matching [Izvekov and Voth()]) is used to coarse grain the MD model into super atoms. Finally after multiple length scales of work, the CG model can be used to make structural predictions. Because of these multiple steps and the need for validation, very few polymer models have been coarse grained. Another set of challenges (not shown here) would be to finegrain the structures determine to form by coarse graining into an atomistic MD model. We did discuss several methods to extract electronic information from MD determined structures, but many of these methods require reintroduction of DFT or other electronic simulation methods. This discussion clearly shows that a reduction in the time and effort required to move between simulation methods would yield a huge increase in the use and predictive power of the methods.

# 4 Conclusions and Recommendations

Understanding structure/property relationships of organic semiconductors requires knowledge of length scales ranging from Angstroms to (at least) microns, and time scales from femtoseconds to milliseconds and beyond. The need for advanced simulation techniques

increases as the experimental toolbox to probe these length and time scales grows. We have shown that DFT and model Hamiltonian based methods give detailed information on electronic behavior, but are limited when model systems increase in size and/or disorder. To simulate larger length and time scales, classical molecular dynamics methods are necessary. Detailed electronic information has to be averaged out to create effective partial charges centered at each atom, which can be a significant source of error in donor–acceptor systems. Molecular dynamics can simulate processes on length and time scales up to 10s of nanometers and microseconds, respectively. This is ideal to study the local arrangements of atoms and local neighborhoods but it is not enough to study self–assembly processes or morphology formation. To achieve necessary length and time scales for that, many groups coarse–grain the atomistic molecular dynamics by grouping atoms into super–atoms, and also often implicitly accounting for solvent molecules. The Iterative Boltzmann Inversion method is commonly used to transition between atomistic and coarse–grained length scales to ensure proper linkage of the larger system to the underlying atomistic system.

Despite the success of each of these methods individually, the key issue moving forward is integrating each of these methods into a consistent multi–scale model and workflow to explain OSCs. The biggest challenge is the transition from quantum chemical to classical atomistic simulations, as there are many examples of OSC systems that do not behave classically even at large length scales. Even structural determination is limited in conjugated samples that have differing partial charge distributions depending on the dihedral angle between conjugated rings. Further development in polarizable and/or reactive force fields is needed to properly transition from the electronic to dynamically adaptive atomistic length scales. Also the fundamentally limiting assumptions in classical simulations insidiously affect the coarse–grained systems as they are parameterized from classical atomistic simulations. The use of polarizable atomistic force fields would also require that the coarse–graining process from atomistic to super–atom systems needs to be generalized to account for polarizability effects.

Multi–scale models are difficult to create for OSCs because we want to understand the electronic behavior at large length scales. We have shown that this typically requires electronic structure methods to parameterize atomistic MD that parameterizes coarse–grained MD. The large–scale morphology is obtained from coarse–grained MD, but we need to synthesize electronic behavior from very limited and often missing data. This is typically achieved through model Hamiltonians or semiclassical theory. However, as we step up the length scale ladder, we loose information or make approximations to increase the simulation volume. If we step down we have to reintroduce information which also requires a set of assumptions. In order to limit these approximations, we identify the adaptive resolution method as an attractive technique for creating multi–scale models for OSCs. The adaptive resolution method is a fascinating development that simultaneously simulates both coarse–grained super-atom and atomistic systems in a consistent way, which provides large scale electrostatics and morphology with atomic scale resolution [Wassenaar *et al.*()Wassenaar, Pluhackova, Böckmann, Marrink, and Tieleman]. This method is being developed to bridge the quantum scale to the atomistic scale through dynamics formulated from path integrals, which can be used to study quantum behavior in a realistic large scale environment [Kreis *et al.*(2014)Kreis, Donadio, Kremer, and Potestio]. Such adaptive resolution techniques can create models that simultaneously simulate all three length scales discussed in this review. However, no model has yet been shown for all three length scales simultaneously, and the atomistic MD still uses non–polarizable

force fields.

Current simulation techniques can still not simultaneously explain multi–length scale experimental data, which inhibits the ability to design new materials, as a clear connection between experiments and molecular design is largely absent. Since the electron–phonon interaction has been identified as critical to the design of OSCs, we see the interface between quantum and classical atomistic simulation techniques as the area most in need of development. Phonon/vibrational modes are commonly simulated using DFT rather than MD because the inter–atomic force constants are not accurately parameterized for vibrational modes. Since electronic behavior is dependent on long range electrostatic interactions, methods that connect coarse-grained morphology to electron dynamics is necessary. Fully understanding electron–phonon interactions and other potential design criteria in the context of molecular design is paramount for the future of molecular simulation of organic electronics.

# References


[Alexiadis and Mavrantzas(2013)] Alexiadis, O. and Mavrantzas, V.G., 2013. All-atom molecular dynamics simulation of temperature effects on the structural, thermodynamic, and packing properties of the pure amorphous and pure crystalline phases of regioregular p3ht, *Macromolecules*, 46 (6), 2450–2467.

[Arias *et al.*(2010)Arias, MacKenzie, McCulloch, Rivnay, and Salleo] Arias, A.C., MacKenzie, J.D., McCulloch, I., Rivnay, J., and Salleo, A., 2010. Materials and applications for large area electronics: Solution-based approaches, *Chemical Reviews*, 110 (1), 3–24.

[Bayramoglu and Faller()] Bayramoglu, B. and Faller, R., . Coarse-grained modeling of polystyrene in various environments by iterative boltzmann inversion.

[Becke(1993)] Becke, A.D., 1993. A new mixing of hartree-fock and local densityâĂŘ-functional theories, *The Journal of Chemical Physics*, 98 (2), 1372–1377.

[Blom *et al.*(2007)Blom, Mihailetchi, Koster, and Markov] Blom, P.W.M., Mihailetchi, V.D., Koster, L.J.A., and Markov, D.E., 2007. Device physics of polymer : fullerene bulk heterojunction solar cells, *Advanced Materials*, 19 (12), 1551–1566.

[Brabec *et al.*(2011)Brabec, Heeney, McCulloch, and Nelson] Brabec, C.J., Heeney, M., McCulloch, I., and Nelson, J., 2011. Influence of blend microstructure on bulk heterojunction organic photovoltaic performance, *Chemical Society Reviews*, 40 (3), 1185–1199.

[Braun *et al.*(2009)Braun, Salaneck, and Fahlman] Braun, S., Salaneck, W.R., and Fahlman, M., 2009. Energy-level alignment at organic/metal and organic/organic interfaces, *Advanced Materials*, 21 (14-15), 1450–1472.

[Breneman and Wiberg(1990)] Breneman, C.M. and Wiberg, K.B., 1990. Determining atom-centered monopoles from molecular electrostatic potentials. the need for high sampling density in formamide conformational analysis, *Journal of Computational Chemistry*, 11 (3), 361–373.

[Brinkmann and Rannou(2009)] Brinkmann, M. and Rannou, P., 2009. Molecular weight dependence of chain packing and semicrystalline structure in oriented films of regioregular poly(3-hexylthiophene) revealed by high-resolution transmission electron microscopy, *Macromolecules*, 42 (4), 1125–1130.

[Chen *et al.*(2012)Chen, Nikiforov, and Darling] Chen, W., Nikiforov, M.P., and Darling, S.B., 2012. Morphology characterization in organic and hybrid solar cells, *Energy & Environmental Science*, 5 (8), 8045–8074.

[Cheng *et al.*(2009)Cheng, Yang, and Hsu] Cheng, Y.J., Yang, S.H., and Hsu, C.S., 2009. Synthesis of conjugated polymers for organic solar cell applications, *Chemical Reviews*, 109 (11), 5868–5923.

[Das and Harrop(2015)] Das, R. and Harrop, P., 2015. Printed, organic & flexible electronics forecasts, players & opportunities 2016-2026, Tech. rep.

[DeLongchamp *et al.*(2012)DeLongchamp, Kline, and Herzing] DeLongchamp, D.M., Kline, R.J., and Herzing, A., 2012. Nanoscale structure measurements for polymer-fullerene photovoltaics, *Energy & Environmental Science*, 5 (3), 5980–5993.

[Di Nuzzo *et al.*(2015)Di Nuzzo, Fontanesi, Jones, Allard, Dumsch, Scherf, Von Hauff, Schumacher, an Di Nuzzo, D., Fontanesi, C., Jones, R., Allard, S., Dumsch, I., Scherf, U., Von Hauff, E., Schumacher, S., and Da Como, E., 2015. How intermolecular geometrical disorder affects the molecular doping of donor-acceptor copolymers, *Nature communications*, 6 (6460).

[Do *et al.*(2010)Do, Huang, Faller, and Moulé] Do, K., Huang, D.M., Faller, R., and Moulé, A.J., 2010. A comparative md study of the local structure of polymer semiconductors p3ht and pbttt, *Phys. Chem. Chem. Phys.*, 12, 14735–14739.

[Du *et al.*(2015)Du, Ji, Xue, Hou, Tang, Lee, and Li] Du, C., Ji, Y., Xue, J., Hou, T., Tang, J., Lee, S.T., and Li, Y., 2015. Morphology and performance of polymer solar cell characterized by DPD simulation and graph theory, *Scientific Reports*, 5, 16854.

[Dudenko *et al.*(2012)Dudenko, Kiersnowski, Shu, Pisula, Sebastiani, Spiess, and Hansen] Dudenko, D., Kiersnowski, A., Shu, J., Pisula, W., Sebastiani, D., Spiess, H.W., and Hansen, M.R., 2012. A strategy for revealing the packing in semicrystalline ĬĂ-conjugated polymers: Crystal structure of bulk poly-3-hexyl-thiophene (p3ht), *Angewandte Chemie International Edition*, 51 (44), 11068–11072.

[Dyakonov and Frankevich(1998)] Dyakonov, V. and Frankevich, E., 1998. On the role played by polaron pairs in photophysical processes in semiconducting polymers, *Chemical Physics*, 227 (1-2), 203–217.

[Eschrig(2003)] Eschrig, H., 2003. *The Fundamentals of Density Functional Theory*, Leipzig, Germany: Edition am Gutenbergplatz.

[Feng *et al.*(2013)Feng, Wang, Zheng, Zhang, Fan, Liu, Amoureux, and Deng] Feng, N., Wang, Q., Zheng, A., Zhang, Z., Fan, J., Liu, S.B., Amoureux, J.P., and Deng, F., 2013. Understanding the high photocatalytic activity of (b, ag)-codoped tio2 under solar-light irradiation with xps, solid-state nmr, and dft calculations, *Journal of the American Chemical Society*, 135 (4), 1607–1616.

[Fornari and Troisi(2014)] Fornari, R.P. and Troisi, A., 2014. Theory of charge hopping along a disordered polymer chain, *Phys. Chem. Chem. Phys.*, 16, 9997–10007.

[Gemünden *et al.*(2013)Gemünden, Poelking, Kremer, Andrienko, and Daoulas] Gemünden, P., Poelking, C., Kremer, K., Andrienko, D., and Daoulas, K.C., 2013. Nematic ordering, conjugation, and density of states of soluble polymeric semiconductors, *Macromolecules*, 46 (14), 5762–5774.

[Gleria and Memming(1976)] Gleria, M. and Memming, R., 1976. Novel luminescence generation by electron-transfer from semiconductor electrodes to ruthenium-bipyridil complexes, *Zeitschrift Fur Physikalische Chemie-Frankfurt*, 101 (1-6), 171–179.

[Goldman *et al.*(2009)Goldman, Reed, Kuo, Fried, Mundy, and Curioni] Goldman, N., Reed, E.J., Kuo, I.F.W., Fried, L.E., Mundy, C.J., and Curioni, A., 2009. Ab initio simulation of the equation of state and kinetics of shocked water, *The Journal of Chemical Physics*, 130 (12), 124517.

[Great Britain. Department for Business and Skills(2009)] Great Britain. Department for Business, I. and Skills, 2009. *Plastic Electronics: A UK strategy for success, Realizing the UK potential*, London.

[Halls *et al.*(1995)Halls, Walsh, Greenham, Marseglia, Friend, Moratti, and Holmes] Halls, J.J.M., Walsh, C.A., Greenham, N.C., Marseglia, E.A., Friend, R.H., Moratti, S.C., and Holmes, A.B., 1995. Efficient photodiodes from interpenetrating polymer networks, *Nature*, 376 (6540), 498–500.

[Hansen *et al.*(2016)Hansen, Graf, and Spiess] Hansen, M.R., Graf, R., and Spiess, H.W., 2016. Interplay of structure and dynamics in functional macromolecular and supramolecular systems as revealed by magnetic resonance spectroscopy, *Chemical Reviews*, 116, 1272–1308.

[Huang *et al.*(2010)Huang, Faller, Do, and Moulé] Huang, D.M., Faller, R., Do, K., and Moulé, A.J., 2010. Coarse-grained computer simulations of polymer/fullerene bulk heterojunctions for organic photovoltaic applications, *Journal of Chemical Theory and Computation*, 6 (2), 526–537.

[Huang *et al.*(2011)Huang, Moulé, and Faller] Huang, D.M., Moulé, A.J., and Faller, R., 2011. Characterization of polymer-fullerene mixtures for organic photovoltaics by systematically coarse-grained molecular simulations, *Fluid Phase Equilibria*, 302 (1-2), 21–25.

[Huang *et al.*(2014)Huang, Kramer, Heeger, and Bazan] Huang, Y., Kramer, E.J., Heeger, A.J., and Bazan, G.C., 2014. Bulk heterojunction solar cells: Morphology and performance relationships, *Chemical Reviews*, 114 (14), 7006–7043.

[Izvekov and Voth()] Izvekov, S. and Voth, G.A., . A multiscale coarse-graining method for biomolecular systems.

[Jankowski *et al.*(2013)Jankowski, Marsh, and Jayaraman] Jankowski, E., Marsh, H.S., and Jayaraman, A., 2013. Computationally linking molecular features of conjugated polymers and fullerene derivatives to bulk heterojunction morphology, *Macromolecules*, 46 (14), 5775–5785.

[Jones *et al.*(2016)Jones, Huang, Chakrabarti, and Groves] Jones, M.L., Huang, D.M., Chakrabarti, B., and Groves, C., 2016. Relating molecular morphology to charge mobility in semicrystalline conjugated polymers, *Journal of Physical Chemistry C*, 120 (8), 4240–4250.

[Kalyani and Dhoble(2012)] Kalyani, N.T. and Dhoble, S.J., 2012. Organic light emitting diodes: Energy saving lighting technology-a review, *Renewable & Sustainable Energy Reviews*, 16 (5), 2696–2723.

[Kayunkid *et al.*(2010)Kayunkid, Uttiya, and Brinkmann] Kayunkid, N., Uttiya, S., and Brinkmann, M., 2010. Structural model of regioregular poly(3-hexylthiophene) obtained by electron diffraction analysis, *Macromolecules*, 43 (11), 4961–4967.

[Ko *et al.*(2012)Ko, Hoke, Pandey, Hong, Mondal, Risko, Yi, Noriega, McGehee, Brédas, Salleo, and B
Ko, S., Hoke, E.T., Pandey, L., Hong, S., Mondal, R., Risko, C., Yi, Y., Noriega, R., McGehee, M.D., Brédas, J.L., Salleo, A., and Bao, Z., 2012. Controlled conjugated backbone twisting for an increased open-circuit voltage while having a high short-circuit current in poly(hexylthiophene) derivatives, *Journal of the American Chemical Society*, 134 (11), 5222–5232.

[Krebs(2009)] Krebs, F.C., 2009. Fabrication and processing of polymer solar cells: A review of printing and coating techniques, *Solar Energy Materials & Solar Cells*, 93 (4, SI), 394–412.

[Krebs *et al.*(2010)Krebs, Nielsen, Fyenbo, Wadstrom, and Pedersen] Krebs, F.C., Nielsen, T.D., Fyenbo, J., Wadstrom, M., and Pedersen, M.S., 2010. Manufacture, integration and demonstration of polymer solar cells in a lamp for the "lighting africa" initiative, *Energy & Environmental Science*, 3 (5), 512–525.

[Kreis *et al.*(2014)Kreis, Donadio, Kremer, and Potestio] Kreis, K., Donadio, D., Kremer, K., and Potestio, R., 2014. A unified framework for force-based and energy-based adaptive resolution simulations, *EPL (Europhysics Letters)*, 108 (3), 30007.

[Lee *et al.*(2015)Lee, Aragó, and Troisi] Lee, M.H., Aragó, J., and Troisi, A., 2015. Charge dynamics in organic photovoltaic materials: Interplay between quantum diffusion and quantum relaxation, *Journal of Physical Chemistry C*, 119 (27), 14989–14998.

[Li *et al.*(2014)Li, Kubis, Forberich, Ameri, Krebs, and Brabec] Li, N., Kubis, P., Forberich, K., Ameri, T., Krebs, F.C., and Brabec, C.J., 2014. Towards large-scale production of solution-processed organic tandem modules based on ternary composites: Design of the intermediate layer, device optimization and laser based module processing, *Solar Energy Materials and Solar Cells*, 120, 701–708.

[Liu *et al.*(2014)Liu, Zhao, Li, Mu, Ma, Hu, Jiang, Lin, Ade, and Yan] Liu, Y., Zhao, J., Li, Z., Mu, C., Ma, W., Hu, H., Jiang, K., Lin, H., Ade, H., and Yan, H., 2014. Aggregation and morphology control enables multiple cases of high-efficiency polymer solar cells, *Nature communications*, 5 (5293).

[Ludwigs(2014)] Ludwigs, S., ed., 2014. *P3HT Revisited: From Molecular Scale to Solar Cell Devices*, vol. 265, Book Series Advances in Polymer Science.

[Marsh *et al.*(2014)Marsh, Jankowski, and Jayaraman] Marsh, H.S., Jankowski, E., and Jayaraman, A., 2014. Controlling the morphology of model conjugated thiophene oligomers through alkyl side chain length, placement, and interactions, *Macromolecules*, 47 (8), 2736–2747.

[Morel *et al.*(1978)Morel, Ghosh, Feng, Stogryn, Purwin, Shaw, and Fishman] Morel, D., Ghosh, A.K., Feng, T., Stogryn, E., Purwin, P., Shaw, R., and Fishman, C., 1978. High-efficiency organic solar cells, *Applied Physics Letters*, 32 (8), 495–497.

[Moulé and Meerholz(2009)] Moulé, A.J. and Meerholz, K., 2009. Morphology control in solution-processed bulk-heterojunction solar cell mixtures, *Advanced Functional Materials*, 19 (19), 3028–3036.

[Müller *et al.*(2008)Müller, Ferenczi, Campoy-Quiles, Frost, Bradley, Smith, Stingelin-Stutzmann, and Müller, C., Ferenczi, T.A.M., Campoy-Quiles, M., Frost, J.M., Bradley, D.D.C., Smith, P., Stingelin-Stutzmann, N., and Nelson, J., 2008. Binary organic photovoltaic blends: A simple rationale for optimum compositions, *Advanced Materials*, 20, 3510–3515.

[Niles *et al.*(2012)Niles, Roehling, Yamagata, Wise, Spano, Moulé, and Grey] Niles, E.T., Roehling, J.D., Yamagata, H., Wise, A.J., Spano, F.C., Moulé, A.J., and Grey, J.K., 2012. J-aggregate behavior in poly-3-hexylthiophene nanofibers, *The Journal of Physical Chemistry Letters*, 3 (2), 259–263.

[Noriega *et al.*(2013)Noriega, Rivnay, Vandewal, Koch, Stingelin, Smith, Toney, and Salleo] Noriega, R., Rivnay, J., Vandewal, K., Koch, F.P.V., Stingelin, N., Smith, P., Toney, M.F., and Salleo, A., 2013. A general relationship between disorder, aggregation and charge transport in conjugated polymers, *Nat Mater*, 12 (11), 1038–1044.

[on Best Practice in National Innovation Programs from Flexible Electronics; National Research Coun on Best Practice in National Innovation Programs from Flexible Electronics; National Research Council, C., 2015. *The Flexible Electronics Opportunity*, Washington, DC: The National Academies Press.

[Paier *et al.*(2005)Paier, Hirschl, Marsman, and Kresse] Paier, J., Hirschl, R., Marsman, M., and Kresse, G., 2005. The perdew-burke-ernzerhof exchange-correlation functional applied to the g2-1 test set using a plane-wave basis set, *The Journal of Chemical Physics*, 122 (23), 234102.

[Peet *et al.*(2009)Peet, Heeger, and Bazan] Peet, J., Heeger, A.J., and Bazan, G.C., 2009. "plastic" solar cells: Self-assembly of bulk heterojunction nanomaterials by spontaneous phase separation, *Accounts of Chemical Research*, 42 (11), 1700–1708.

[Poelking and Andrienko(2013)] Poelking, C. and Andrienko, D., 2013. Effect of polymorphism, regioregularity and paracrystallinity on charge transport in poly(3-hexylthiophene) [p3ht] nanofibers, *Macromolecules*, 46 (22), 8941–8956.

[Poelking *et al.*(2014)Poelking, Daoulas, Troisi, and Andrienko] Poelking, C., Daoulas, K., Troisi, A., and Andrienko, D., 2014. *Morphology and Charge Transport in P3HT: A Theorist's Perspective*, Berlin, Heidelberg: Springer Berlin Heidelberg, 139–180.

[Poelking *et al.*(2015)Poelking, Tietze, Elschner, Olthof, Hertel, Baumeier, Wuerthner, Meerholz, Leo, Poelking, C., Tietze, M., Elschner, C., Olthof, S., Hertel, D., Baumeier, B., Wuerthner, F., Meerholz, K., Leo, K., and Andrienko, D., 2015. Impact of mesoscale order on open-circuit voltage in organic solar cells, *Nature Materials*, 14 (4), 434–439.

[Praprotnik *et al.*(2008)Praprotnik, Delle Site, and Kremer] Praprotnik, M., Delle Site, L., and Kremer, K., 2008. *Multiscale simulation of soft matter: From scale bridging to adaptive resolution*, *Annual Review of Physical Chemistry*, vol. 59, 545–571.

[Prosa *et al.*(1992)Prosa, Winokur, Moulton, Smith, and Heeger] Prosa, T.J., Winokur, M.J., Moulton, J., Smith, P., and Heeger, A.J., 1992. X-ray structural studies of poly(3-alkylthiophenes): an example of an inverse comb, *Macromolecules*, 25 (17), 4364–4372.

[Pynn(2009)] Pynn, R., 2009. *Neutron Scattering–A Non-destructive Microscope for Seeing Inside Matter*, Springer.

[Rivnay *et al.*(2012)Rivnay, Mannsfeld, Miller, Salleo, and Toney] Rivnay, J., Mannsfeld, S.C.B., Miller, C.E., Salleo, A., and Toney, M.F., 2012. Quantitative determination of organic semiconductor microstructure from the molecular to device scale, *Chemical Reviews*, 112 (10), 5488–5519.

[Roehling *et al.*(2013)Roehling, Batenburg, Swain, Moulé, and Arslan] Roehling, J.D., Batenburg, K.J., Swain, F.B., Moulé, A.J., and Arslan, I., 2013. Three-dimensional concentration mapping of organic blends, *Advanced Functional Materials*, 23 (17), 2115–2122.

[Root *et al.*(2016)Root, Savagatrup, Pais, Arya, and Lipomi] Root, S.E., Savagatrup, S., Pais, C.J., Arya, G., and Lipomi, D.J., 2016. Predicting the mechanical properties of organic semiconductors using coarse-grained molecular dynamics simulations, *Macromolecules*, 49 (7), 2886–2894.

[Salleo *et al.*(2010)Salleo, Kline, DeLongchamp, and Chabinyc] Salleo, A., Kline, R.J., DeLongchamp, D.M., and Chabinyc, M.L., 2010. Microstructural characterization and charge transport in thin films of conjugated polymers, *Advanced Materials*, 22 (34), 3812–3838.

[Sasabe and Kido(2011)] Sasabe, H. and Kido, J., 2011. Multifunctional materials in high-performance oleds: Challenges for solid-state lighting, *Chemistry of Materials*, 23 (3), 621–630.

[Schwarz *et al.*(2013)Schwarz, Kee, and Huang] Schwarz, K.N., Kee, T.W., and Huang, D.M., 2013. Coarse-grained simulations of the solution-phase self-assembly of poly(3-hexylthiophene) nanostructures, *Nanoscale*, 5, 2017–2027.

[Schweicher *et al.*(2015)Schweicher, Lemaur, Niebel, Ruzie, Diao, Goto, Lee, Kim, Arlin, Karpinska, K Schweicher, G., Lemaur, V., Niebel, C., Ruzie, C., Diao, Y., Goto, O., Lee, W.Y., Kim, Y., Arlin, J.B., Karpinska, J., Kennedy, A.R., Parkin, S.R., Olivier, Y., Mannsfeld, S.C.B., Cornil, J., Geerts, Y.H., and Bao, Z., 2015. Bulky end-capped 1 benzothieno 3,2-b benzothiophenes: Reaching high-mobility organic semiconductors by fine tuning of the crystalline solid-state order, *Advanced Materials*, 27 (19), 3066–3072.

[Sha and Faller(2016)] Sha, H. and Faller, R., 2016. A quantum chemistry study of curvature effects on boron nitride nanotubes/nanosheets for gas adsorption, *Phys. Chem. Chem. Phys.*, 18, 19944–19949.

[Sirringhaus(2014)] Sirringhaus, H., 2014. 25th anniversary article: Organic field effect transistors: The path beyond amorphous silicon, *Advanced materials*, (9), 1319–1335.

[Spano(2005)] Spano, F.C., 2005. Modeling disorder in polymer aggregates: The optical spectroscopy of regioregular poly(3-hexylthiophene) thin films, *The Journal of Chemical Physics*, 122 (23), 234701.

[Sun *et al.*(2008)Sun, Ghosh, and Faller] Sun, Q., Ghosh, J., and Faller, R., 2008. *Coarse–Graining of Condensed Phase and Biomolecular Systems*, CRC Press, chap. State Point Dependence and Transferability of Potentials in Systematic Structural Coarse–Graining, 69–82.

[Tapping *et al.*(2015)Tapping, Clafton, Schwarz, Kee, and Huang] Tapping, P.C., Clafton, S.N., Schwarz, K.N., Kee, T.W., and Huang, D.M., 2015. Molecular-level details of morphology-dependent exciton migration in poly(3-hexylthiophene) nanostructures, *The Journal of Physical Chemistry C*, 119 (13), 7047–7059.

[Usta *et al.*(2011)Usta, Facchetti, and Marks] Usta, H., Facchetti, A., and Marks, T.J., 2011. n-channel semiconductor materials design for organic complementary circuits, *Accounts of Chemical Research*, 44 (7), 501–510.

[Vanlaeke *et al.*(2006)Vanlaeke, Swinnen, Haeldermans, Vanhoyland, Aernouts, Cheyns, Deibel, D'Hae Vanlaeke, P., Swinnen, A., Haeldermans, I., Vanhoyland, G., Aernouts, T., Cheyns, D., Deibel, C., D'Haen, J., Heremans, P., Poortmans, J., and Manca, J., 2006. P3ht/pcbm bulk heterojunction solar cells: Relation between morphology and electro-optical characteristics, *Solar Energy Materials and Solar Cells*, 90 (14), 2150 – 2158.

[Venkateshvaran *et al.*(2014)Venkateshvaran, Nikolka, Sadhanala, Lemaur, Zelazny, Kepa, Hurhangee, Venkateshvaran, D., Nikolka, M., Sadhanala, A., Lemaur, V., Zelazny, M., Kepa, M., Hurhangee, M., Kronemeijer, A.J., Pecunia, V., Nasrallah, I., Romanov, I., Broch, K., McCulloch, I., Emin, D., Olivier, Y., Cornil, J., Beljonne, D., and Sirringhaus, H., 2014. Approaching disorder-free transport in high-mobility conjugated polymers, *Nature*, 515 (7527), 384–388.

[Wassenaar *et al.*()Wassenaar, Pluhackova, Böckmann, Marrink, and Tieleman] Wassenaar, T.A., Pluhackova, K., Böckmann, R.A., Marrink, S.J., and Tieleman, D.P., .

[Winokur *et al.*(1989)Winokur, Spiegel, Kim, Hotta, and Heeger] Winokur, M., Spiegel, D., Kim, Y., Hotta, S., and Heeger, A., 1989. Structural and absorption studies of the thermochromic transition in poly(3-hexylthiophene), *Synthetic Metals*, 28 (1), 419 – 426.

[Yanai *et al.*(2004)Yanai, Tew, and Handy] Yanai, T., Tew, D.P., and Handy, N.C., 2004. A new hybrid exchange correlation functional using the coulomb-attenuating method (cam-b3lyp), *Chemical Physics Letters*, 393 (1-3), 51 – 57.

[Yang *et al.*(2005)Yang, Loos, Veenstra, Verhees, Wienk, Kroon, Michels, and Janssen] Yang, X.N., Loos, J., Veenstra, S.C., Verhees, W.J.H., Wienk, M.M., Kroon, J.M., Michels, M.A.J., and Janssen, R.A.J., 2005. Nanoscale morphology of high-performance polymer solar cells, *Nano Letters*, 5 (4), 579–583.

[Yin *et al.*(2016)Yin, Wang, Fazzi, Shen, and Soci] Yin, J., Wang, Z., Fazzi, D., Shen, Z., and Soci, C., 2016. First-principles study of the nuclear dynamics of doped conjugated polymers, *The Journal of Physical Chemistry C*, 120 (3), 1994–2001.

[Yin and Dadmun(2011)] Yin, W. and Dadmun, M., 2011. A new model for the morphology of p3ht/pcbm organic photovoltaics from small-angle neutron scattering: Rivers and streams, *ACS Nano*, 5 (6), 4756–4768.

[Yu *et al.*(1995)Yu, Gao, Hummelen, Wudl, and Heeger] Yu, G., Gao, J., Hummelen, J.C., Wudl, F., and Heeger, A.J., 1995. Polymer photovoltaic cells - enhanced efficiencies via a network of internal donor-acceptor heterojunctions, *Science*, 270 (5243), 1789–1791.

[Yuan *et al.*()Yuan, Zhang, Sun, Hu, Zhang, and Duan] Yuan, Y., Zhang, J., Sun, J., Hu, J., Zhang, T., and Duan, Y., .

[Zahn *et al.*(2007)Zahn, Gavrila, and Salvan] Zahn, D.R.T., Gavrila, G.N., and Salvan, G., 2007. Electronic and vibrational spectroscopies applied to organic/inorganic interfaces, *Chemical Reviews*, 107 (4), 1161–1232.

[Zhang *et al.*(2016)Zhang, Ye, and Hou] Zhang, S., Ye, L., and Hou, J., 2016. Breaking the 10% efficiency barrier in organic photovoltaics: Morphology and device optimization of well-known pbdttt polymers, *Advanced Energy Materials*, 6 (11), 1502529.

[Zhu *et al.*(2011)Zhu, Kim, Yi, and Brédas] Zhu, L., Kim, E.G., Yi, Y., and Brédas, J.L., 2011. Charge transfer in molecular complexes with 2,3,5,6-tetrafluoro-7,7,8,8-tetracyanoquinodimethane (f4-tcnq): A density functional theory study, *Chemistry of Materials*, 23 (23), 5149–5159.